Science Bulletin 64 (2019) 1215–1221

Contents lists available at ScienceDirect

Science Bulletin

journal homepage: www.elsevier.com/locate/scib

Article

Experimental evidence of anomalously large superconducting gap on topological surface state of β-Bi_2Pd film

Jian-Yu Guan [a,b,1], Lingyuan Kong [a,b,1], Li-Qin Zhou [a,b], Yi-Gui Zhong [a,b], Hang Li [a,b], Hai-Jiang Liu [a,b], Cen-Yao Tang [a,b], Da-Yu Yan [a,b], Fa-Zhi Yang [a,b], Yao-Bo Huang [c], You-Guo Shi [a,e], Tian Qian [a,d,e], Hong-Ming Weng [a,e], Yu-Jie Sun [a,d,e,*], Hong Ding [a,d,e,*]

[a] Beijing National Laboratory for Condensed Matter Physics and Institute of Physics, Chinese Academy of Sciences, Beijing 100190, China
[b] School of Physics, University of Chinese Academy of Sciences, Beijing 100190, China
[c] Shanghai Synchrotron Radiation Facility, Shanghai Institute of Applied Physics, Chinese Academy of Sciences, Shanghai 201204, China
[d] CAS Center for Excellence in Topological Quantum Computation, University of Chinese Academy of Sciences, Beijing 100190, China
[e] Songshan Lake Materials Laboratory, Dongguan 523808, China

ARTICLE INFO

Article history:
Received 4 June 2019
Received in revised form 3 July 2019
Accepted 12 July 2019
Available online 19 July 2019

Keywords:
Topological surface state
Multiband superconductivity
Thin film
Photoemission spectroscopy

ABSTRACT

Connate topological superconductor (TSC) combines topological surface states with nodeless superconductivity in a single material, achieving effective p-wave pairing without interface complication. By combining angle-resolved photoemission spectroscopy and in-situ molecular beam epitaxy, we studied the momentum-resolved superconductivity in β-Bi_2Pd film. We found that the superconducting gap of topological surface state ($\Delta_{TSS} \sim 3.8$ meV) is anomalously enhanced from its bulk value ($\Delta_b \sim 0.8$ meV). The ratio of $2\Delta_{TSS}/k_BT_c \sim 16.3$, is substantially larger than the BCS value. By measuring β-Bi_2Pd bulk single crystal as a comparison, we clearly observed the upward-shift of chemical potential in the film. In addition, a concomitant increasing of surface weight on the topological surface state was revealed by our first principle calculation, suggesting that the Dirac-fermion-mediated parity mixing may cause this anomalous superconducting enhancement. Our results establish β-Bi_2Pd film as a unique case of connate TSCs with a highly enhanced topological superconducting gap, which may stabilize Majorana zero modes at a higher temperature.

1. Introduction

The studies of superconducting (SC) topological surface states [1] have been propelled by the prospect of harboring vortex-confined Majorana zero mode (MZM) [2,3], which is widely believed to be a building block of fault-tolerant quantum computation [4]. Theoretically, MZMs can emerge as a special type of Bogoliubov excitations in an intrinsic topological superconductor (TSC) with p-wave pairing [5,6], or in artificial designs combing conventional s-wave superconductivity with special band structures [1,7–27], e.g., the topological insulating states [1,7–9,16,20–22]. In the latter case, a superconducting topological surface state has been proved to play a similar role as a two-dimensional p-wave superconductor [1,2]. An effective p-wave superconductivity can be realized on the interface of a proximitized heterostructure between an s-wave superconductor and a strong topological insulator (TI) [16,20–22], or on the sample surface of a self-proximitized connate TSC [28–53], i.e., a full-gapped bulk superconductor holds topological surface states [47,51]. Heterostructures usually suffer shortcomings such as gap softness [54,55] and fragile device fabrication [26,27], thus are difficult for observing and manipulating MZMs in experiments [55,56]. It has been a long sought-after goal to find an ideal platform which can easily create, measure and control MZMs. Recently, topological surface states and MZMs are observed clearly in single material platforms of Fe(Te,Se) bulk single crystals [38–50] and similar compounds of iron-based superconductors [49,51–53], which indicates that a connate TSC is a promising platform for pursuing topological quantum computation [47].

The SC gap of topological surface state (Δ_{TSS}) plays a vital role in protecting MZM that a larger Δ_{TSS} leads to a larger energetic separation between MZM and other trivial excitations [2,43,44]. In general, Δ_{TSS} of a surface state is smaller than the SC gap of bulk bands (Δ_b), due to the proximitized pairing amplitude decays from bulk to surface. Interestingly, a special candidate of connate TSC, β-Bi_2Pd film, may break this rule [34–36]. A previous scanning

* Corresponding authors.
E-mail addresses: yjsun@iphy.ac.cn (Y.-J. Sun), dingh@iphy.ac.cn (H. Ding).
[1] These authors contributed equally to this work.

https://doi.org/10.1016/j.scib.2019.07.019
2095-9273/

tunneling microscopy/spectroscopy (STM/S) experiment found two SC gaps ($\Delta_1 \sim 1.0$ meV and $\Delta_2 \sim 3.3$ meV) in the β-Bi_2Pd film grown by molecular beam epitaxy [35], while only the smaller one (Δ_1) compares to the SC gap of β-Bi_2Pd bulk single crystal ($\Delta_b \sim 0.8$ meV, $T_c = 5.4$ K) [36,57,58]. Large zero-bias conductance peaks (ZBCPs) were observed in the line-cut measurement across its SC vortices. The ZBCPs do not split within a certain length from the vortex center, which indicates certain mixtures of MZMs inside the intensity of ZBCPs [35]. Consequently, the anomalous large gap (Δ_2) was attributed to the enhanced Δ_{TSS} of the topological surface state, but the direct momentum-resolving evidence is still absent [35,59]. In this work, we performed angle-resolved photoemission spectroscopy (ARPES) measurements on as-grown β-Bi_2Pd thin film to directly resolve the origin of the large gap Δ_2 [35]. We found the experimental evidences of an anomalously large SC gap at the Fermi-momentum (k_F) of topological surface state which likely corresponds to Δ_2. On the contrary, no such large SC gap can be found in neither the trivial surface state nor the bulk bands. By comparing with bulk single crystal, we showed that the chemical potential is shifted upward in the film, which might be the cause of the deviation between different types of samples.

2. Methods

The (001)-oriented 20-UC β-Bi_2Pd thin films were epitaxially grown on Nb-doped (0.7 wt%) $SrTiO_3$(001) substrates at ~ 320 °C. High-purity Bi (99.9999%) and Pd (99.99%) sources were co-evaporated from Knudsen cells with a flux ratio of 5.3, which were measured by a quartz crystal monitor. Films were studied in-situ using home-made room-temperature STM and low-temperature ARPES with ultrahigh vacuum better than 3.0×10^{-11} Torr (1 Torr $\approx$ 133.322 Pa). The ARPES system is equipped with a Scienta R4000 analyzer and a helium discharge lamp with He-Iα photons (21.218 eV). The energy resolution was set ~ 3 meV for gap measurements and ~ 7 meV for band structure measurements. The angular resolution was set to $\sim 0.2°$. ARPES measurements on β-Bi_2Pd bulk single crystals with 20 eV photons were performed at

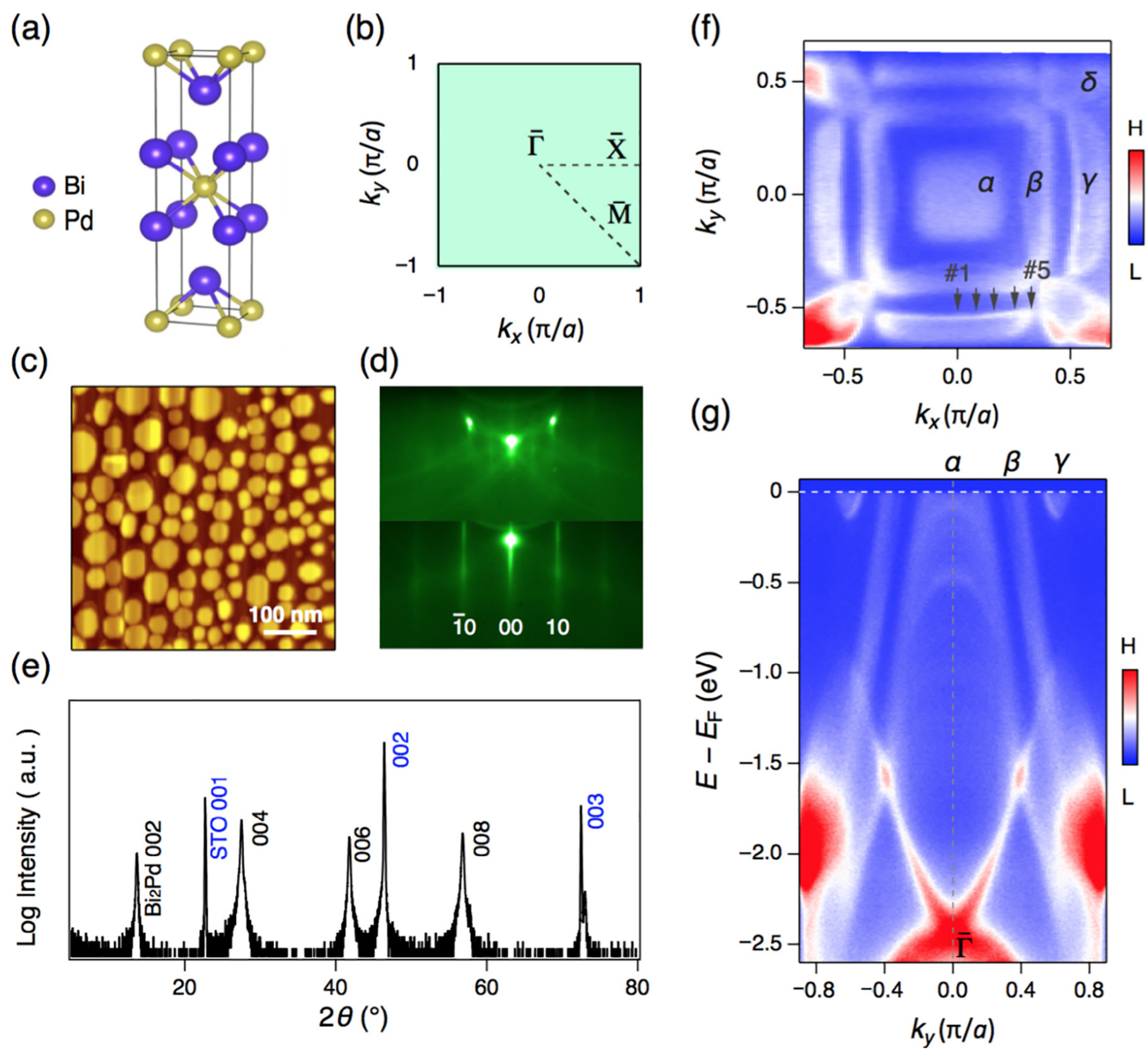

Fig. 1. (Color online) Crystal and electronic structure of the β-Bi_2Pd film. (a) Crystal structure of tetragonal β-Bi_2Pd film. Layers are stacked by van der Waals interaction. Each unit cell (UC) is made up of two Bi-Pd-Bi triple layers. (b) Projected surface Brillouin zone with high symmetry points ($\bar{\Gamma}$, $\bar{M}$ and $\bar{X}$). (c) Constant-current STM topographic image of as-grown 20-UC β-Bi_2Pd film (setpoint voltage: $V_s = 2.13$ V, tunneling current: $I_t = 270$ pA, 500 nm $\times$ 500 nm). (d) Reflection high-energy electron diffraction pattern taken from the (001) surface on an annealed $SrTiO_3$ substrate (top panel) and that of β-Bi_2Pd film with Kikuchi lines formed by inelastically scattered electrons (bottom panel), indicating high crystalline coherence. (e) X-ray diffraction spectrum taken from the same film illustrates lattice constant $c = 12.97$ Å (X-rays with wavelength 1.54 Å). (f) Four-fold symmetrized Fermi surface obtained by ARPES at 20 K shows spectral weight within $E_F \pm 10$ meV. The Fermi surface is composed of two hole bands (α, β) and two electron bands (γ, δ). Black arrows with numbers #1 to #5 mark the positions of the cuts shown in Fig. 2e. (g) Large-range ARPES spectrum observed along $\bar{\Gamma} - \bar{X}$.

the “Dreamline” beamline of the Shanghai Synchrotron Radiation Facility (SSRF) with a Scienta DA30 analyzer.

3. Results and discussion

The 20-UC β-Bi_2Pd thin films measured in this work have tetragonal structure (space group *I4/mmm*) (Fig. 1a). The lattice mismatch between substrate and β-Bi_2Pd is released as growing layer-by-layer. Lattice constants of thin film are $a = b = 3.41$ Å, $c = 12.97$ Å, obtained by in-situ reflection high-energy electron diffraction measurement (bottom panel of Fig. 1d) and X-ray diffraction (XRD) (Fig. 1e), which are in good agreement with the bulk single crystal. A STM image of the film (Fig. 1c) shows patch-like growing nature of β-Bi_2Pd, which is consistent with previous STM study that observed two SC gaps [35]. Our XRD measurements show (001)-oriented single crystallization of thin films. We performed ARPES measurements on these films with He-Iα photons. Similar as the results of the bulk single crystal [34], four-fold symmetric Fermi surfaces with four Fermi pockets are resolved (Fig. 1f). The band dispersion along $\bar{\Gamma}-\bar{X}$ (Fig. 1b) is plotted in Fig. 1g, with two hole-like bands (α, β) and one electron-like band (γ) crossing the Fermi level (E_F).

It has been resolved in β-Bi_2Pd bulk single crystal that a surface Dirac cone appears beneath the α band [34], with the binding energy of the Dirac point around −2.4 eV. It is known that in a thin film of TI within only a few layers, the topological surface states on the two sides may strongly hybridize with each other, leading to gap opening at the Dirac point [60,61]. An ideal TI preserving topological protection should be free of such a hybridization gap. We checked the spectra of high binding energy between −1.4 and −3 eV in our measurements. A clear Dirac dispersion (Fig. 2a) with isotropic constant-energy contours (Fig. 2b) can be observed, suggesting that our 20-UC thin film keeps the topological surface states intact and is similar to the bulk material [34].

Next, we turn to the surface states near E_F. We display ARPES dispersion near E_F along $\bar{\Gamma}-\bar{X}$ (Fig. 2c). Besides the bulk bands mentioned before (Fig. 1g), there are two distinguishable surface states observed in our measurements. According to previous experiments [34] and our first principle calculation, we clearly identify those bands as a trivial surface state (β') deriving from the β band and a topological surface state (γ') connecting the β and γ bands. Remarkably, there is an obvious dip between γ' and γ bands in the momentum distribution curve (MDC) extracted at E_F (the red curve appended in Fig. 2c), which is more distinct in the film as comparing to the previous study on the bulk single crystal [34]. The separation between the topological surface states and the bulk bands is clearly demonstrated in a curvature intensity plot around the γ' and γ bands (Fig. 2d). It leads us to conjecture that more surface state components are presented in the film materials, which preserves the topological properties from overlapping with other bulk signals. We display five cuts along k_y (Fig. 2e), with their k_x positions indicated in Fig. 1f. The Fermi-level MDCs show γ' gradually merges into γ, when moving from the Brillouin zone center (cut#1) to the edge (cut#5) (Fig. 2f). It implies that the surface components reach the maximum at $\bar{\Gamma}-\bar{X}$, which is the best place to study the intrinsic superconductivity of topological surface state (γ') in the films.

Next, we focus on the momentum-resolved superconductivity of β-Bi_2Pd film. We performed high-resolution ARPES measurements along $\bar{\Gamma}-\bar{X}$ under different temperatures, i.e., below T_c (2.7 K) (Fig. 3a) and above T_c (20 K) (Fig. 3b). We notice that the topological surface state (γ') bends toward higher binding energy when k approaches k_F at 2.7 K (Fig. 3a), while the band straightly crosses E_F at 20 K (Fig. 3b). This behavior implies the formation of a SC gap. The bending back feature is a characteristic of Bogoliubov dispersion of SC state. The Bogoliubov quasiparticles produce a sharp coherent peak and its position can be defined as the size of SC gap [62–68]. We extracted energy distribution curves (EDCs) at three representative momenta, namely k_1, k_2 and k_3 (as marked in Fig. 2c), which correspond to the k_F values of topological surface state (γ'), trivial surface state (β') and bulk state (α), respectively. Surprisingly, at k_1, the EDC measured at 2.7 K shows a sharp peak

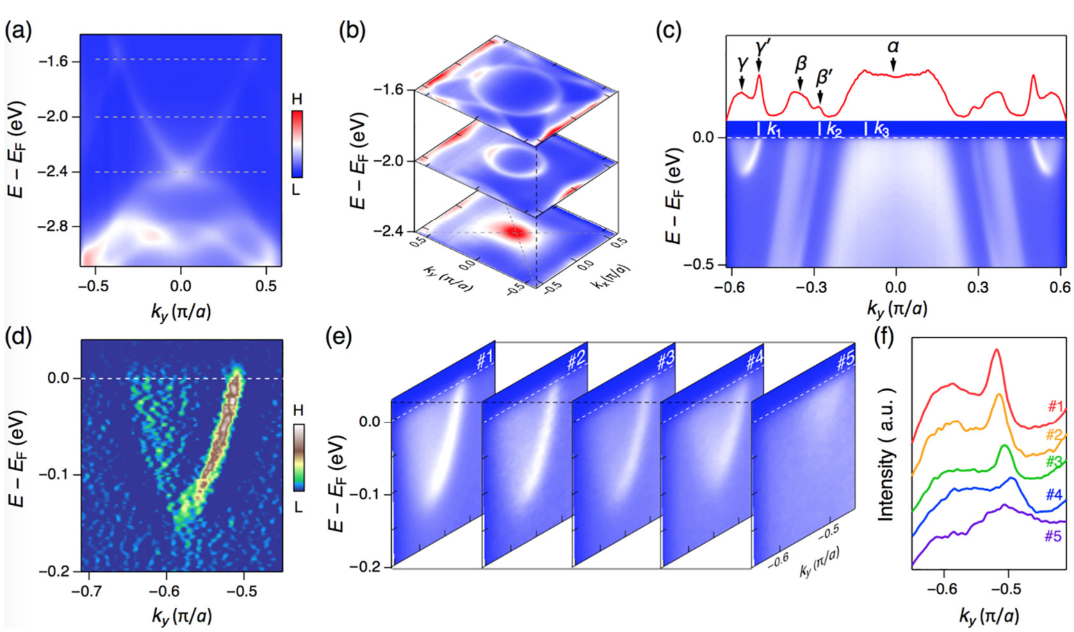

Fig. 2. (Color online) Surface states of the β-Bi_2Pd film. (a) High binding energy band dispersion of 20-UC β-Bi_2Pd film. An intact surface Dirac cone dispersion along $\bar{\Gamma}-\bar{X}$. (b) Constant energy contours at binding energy E_D, E_D + 0.4 eV and E_D + 0.8 eV, where E_D (−2.4 eV) is the energy of the Dirac point. (c) Close-up of ARPES spectrum (along $\bar{\Gamma}-\bar{X}$) near E_F measured at 20 K. The topological surface state γ' connects the γ and β bulk states, and the trivial surface state β' derived from the bulk state β. The red line represents the extracted momentum distribution curve (MDC) at E_F. Three representative momenta, namely k_1, k_2 and k_3, correspond to the Fermi momentum of γ', β' and α bands, respectively. (d) Curvature intensity plot of the γ and γ' bands. (e) Momentum dependence of the γ and γ' dispersions, k_x positions of cuts #1 to #5 are indicated in Fig. 1f. (f) MDCs extracted at E_F for the five cuts, offset for clarity.

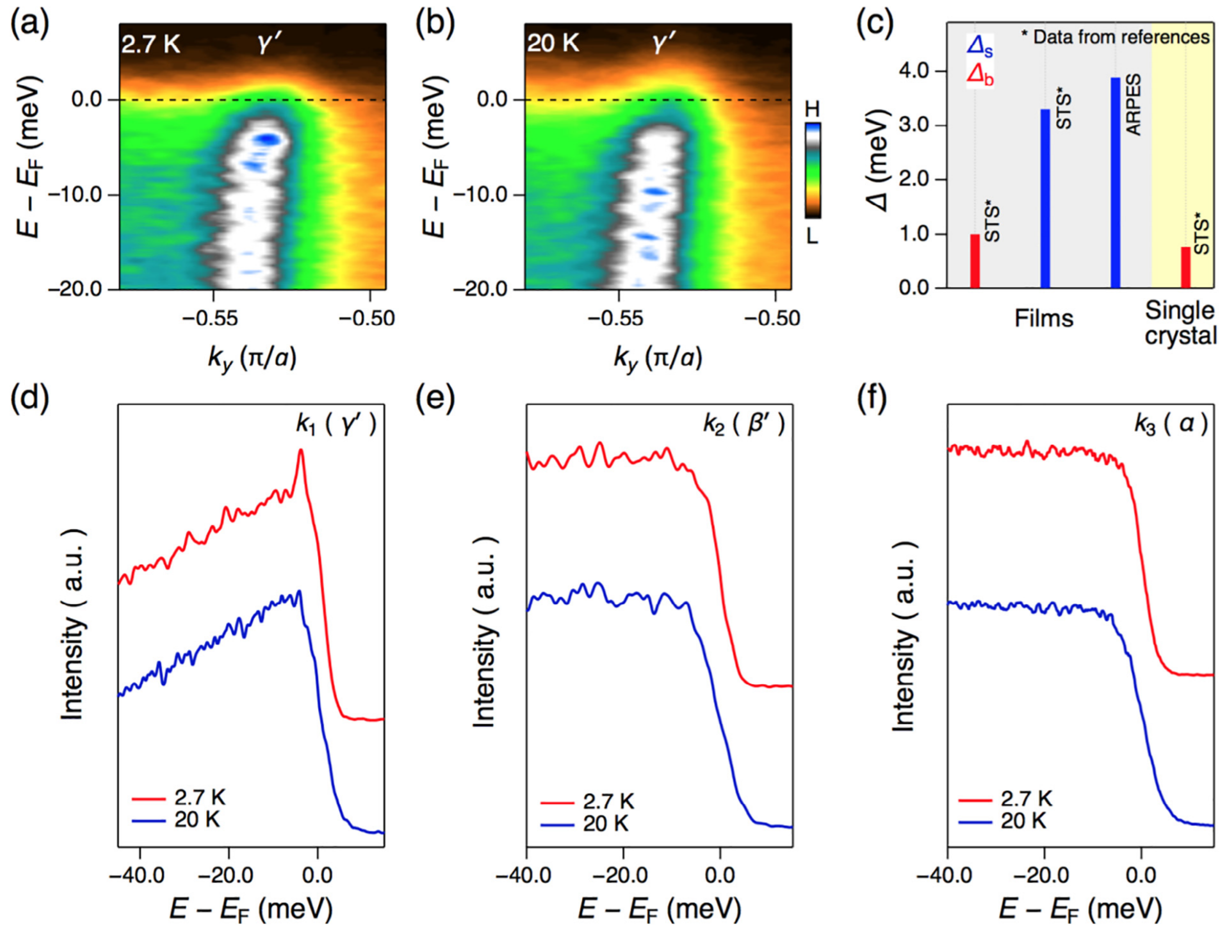

Fig. 3. (Color online) Temperature dependence on surface and bulk state of β-Bi_2Pd film. Close-up of ARPES spectra near E_F along $\bar{\Gamma}-\bar{X}$ measured on the topological surface state (γ') at 2.7 K (a) and 20 K (b), respectively. (c) A collection of SC gaps measured on β-Bi_2Pd samples. Red (blue) color represents the size of SC gap on the topological surface state Δ_s (bulk band Δ_b). The SC gap measured on bulk single crystal is about 0.8 meV measured by scanning tunneling spectroscopy (STS) [36,57]. The SC gap values measured on the film in previous STM experiments [35] are 1 meV (Δ_1) and 3.3 meV (Δ_2), which are assigned as SC gap on bulk bands and topological surface states, respectively. The SC gap measured on the topological surface state in this work is 3.8 meV. (d) The energy distribution curves (EDCs) are extracted on the momentum k_1 (topological surface state) at 2.7 K (red curve) and 20 K (blue curve). (e) and (f) are same as (d) but measured on momenta k_2 (trivial surface state) and k_3 (bulk state), respectively.

at −3.8 meV (the red curve in Fig. 3d), which was in contrast with the featureless EDC measured at 20 K (the blue curve in Fig. 3d). We attributed this sharp peak as the enhanced SC gap as measured in the previous STM/S study ($\Delta_2 \sim 3.3$ meV) [35]. These observations were reproduced several times in different samples (see Supplementary data), which strengthens us confidence of the existence of SC topological surface states in β-Bi_2Pd films with an anomalously large SC gap. We notice that the EDCs measured on the k_F of trivial surface state (Fig. 3e) and bulk band (Fig. 3f) are featureless near E_F, even at 2.7 K. This observation is reasonable because the SC gap values of those bands ($\Delta_1 \sim 1$ meV of films [35] and $\Delta_b \sim 0.8$ meV of bulk single crystal [36,57]) are much smaller than the experimental energy resolution of our ARPES system (∼ 3 meV). We summarize the gap sizes measured by different techniques in Fig. 3c, and the SC gap measured in this work is comparable to previous STM/S observations [35]. The appearance of two classes of SC gaps indicates the paring potential is indeed enhanced on the topological surface states.

In order to resolve the puzzle of the anomalous SC gap enhancement on the topological surface state in this film material, we conducted comparison studies between 20-UC films and bulk single crystals of β-Bi_2Pd. We observed that the chemical potential shifts upward about 37 meV in the thin film (Fig. 4a). We repeated this measurement for several times on different samples and obtained confirming results (see Supplementary data). Theoretically, the odd and even components of the SC order parameter can mix with each other on the sample surface due to inversion symmetry broken [69]. A similar phenomenon of enhanced Δ_{TSS} was proposed in $Cu_xBi_2Se_3$ previously [70], that the orbital polarization of topological surface states leads to constructive parity mixing of SC order parameters. However, the trivial surface states cannot support such constructive mixing, although odd and even components of the order parameter do coexist on the surface [70,71]. It was suggested that a larger Fermi momentum separation (δ_k) between topological surface states and adjacent bulk band, equivalently a larger surface weight of topological surface states, can lead to a stronger enhancement of Δ_{TSS} [70]. However, the δ_k difference between thin film and bulk single crystal is not quite clear in our experiment. So that we performed a slab calculation to simulate the surface weight of topological surface states at different chemical potentials (see Supplementary data). The calculated band structure is consistent with our experimental results and previous studies [34,72]. The color scale in Fig. 4b indicates the surface weight. Apparently, the surface weight becomes larger when the chemical potential is increased (inset of Fig. 4b). Although our calculation qualitatively supports the mechanism of Dirac-Fermion-

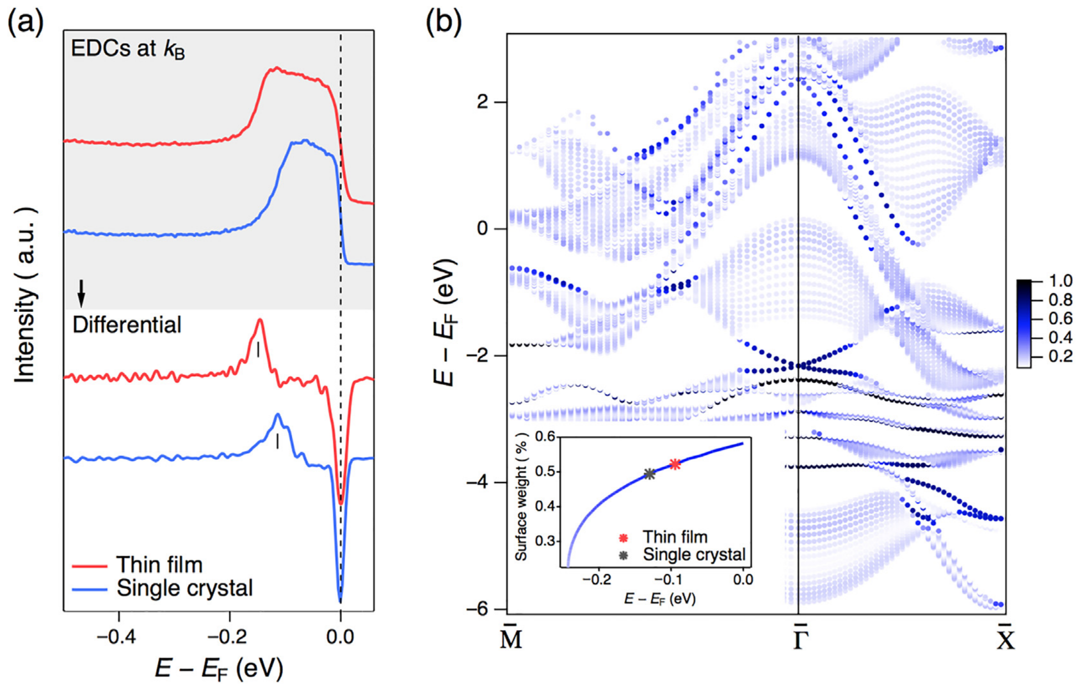

Fig. 4. (Color online) Upward chemical potential in the β-Bi_2Pd film and calculated surface state weight by slab calculation. (a) EDCs at k_B taken from a bulk single crystal (blue curve) and a film (red curve) where k_B represents the momentum of the γ band bottom (top panel). We define the binding energy of the band bottom by the peaks of first derivative of the EDCs (bottom panel). The chemical potential of the thin film shifts upward ~37 meV as comparing with the bulk single crystal. (b) The projection of (001) surface bands obtained by slab calculation of 11 Bi_2Pd layers. The color scale indicates the weight of surface component. The inset shows the surface weight of γ' (blue curve). The position of the chemical potential for the thin film (the bulk single crystal) as marked by red (grey) dot.

mediated parity mixing [70] in explaining Δ_{TSS} enhancement, the surface weight difference between bulk single crystal and thin film is only ~6%. Thus we caution on how such a small change could lead to this large enhancement of SC gap. A realistic model or a different mechanism may be needed in order to resolve this puzzle.

4. Conclusion

In conclusion, we performed in-situ ARPES measurements on β-Bi_2Pd films and bulk single crystals. We observed a direct momentum-resolved evidence of an anomalously large SC gap on its topological surface state. A possible enhancing mechanism, which is the Dirac-Fermion-mediated parity mixing [71], was discussed based on our observation of chemical potential shift and the concomitant increasing of surface weight revealed in our first principle calculations.

Conflict of interest

The authors declare that they have no conflict of interest.

Acknowledgments

This work at IOP was supported by the Ministry of Science and Technology of China, China (2016YFA0401000, 2016YFA0300600, 2015CB921000), the National Natural Science Foundation of China, China (11888101, 11574371, 11622435, 11474340 and 11774399), the Chinese Academy of Sciences, China (XDB28000000, XDB07000000, QYZDB-SSW-SLH043), the Beijing Municipal Science and Technology Commission, China (Z171100002017018, Z181100004218005 and Z171100002017018), Beijing Natural Science Foundation (Z180008), and the National Key Research and Development Program of China, China (2017YFA0302901), Y.-B. H. acknowledges supports by the Ministry of Science and Technology of China, China (2016YFA0401002) and the CAS Pioneer "Hundred Talents Program" (type C). The authors also thank C. Fang for useful discussions.

Author contributions

H.D. and Y.-J. S. designed the experiments and supervised the project. J.-Y. G. and Y.-J. S. grew the thin films and performed STM, RHEED and XRD measurements. L.-Y. K. and J.-Y. G. performed ARPES measurements with the assistance of H. Li., Y.-G. Z., H.-J. L., C.-Y. T., F.-Z. Y., Y.-B. H. and T. Q. D.-Y. Y. and Y.-G. S. provided high quality bulk single crystals. L.-Q. Z. and H.-M. W. performed first principle calculation. J.-Y. G. and L.-Y. K. analysed the ARPES data. J.-Y. G. plotted the figures. L.-Y. K., J.-Y. G., Y.-J. S. and H. D. wrote the manuscripts with inputs from all the authors.

Appendix A. Supplementary data

Supplementary data to this article can be found online at https://doi.org/10.1016/j.scib.2019.07.019.

References

[1] Fu L, Kane CL. Superconducting proximity effect and Majorana fermions at the surface of a topological insulator. Phys Rev Lett 2008;100:096407.
[2] Alicea J. New directions in the pursuit of Majorana fermions in solid state systems. Rep Prog Phys 2012;75:076501.
[3] Elliott SR, Franz M. *Colloquium*: Majorana fermions in nuclear, particle, and solid-state physics. Rev Mod Phys 2015;87:137.
[4] Nayak C, Simon SH, Stern A, et al. Non-Abelian anyons and topological quantum computation. Rev Mod Phys 2008;80:1083–159.
[5] Read N, Green D. Paired states of fermions in two dimensions with breaking of parity and time-reversal symmetries and the fractional quantum Hall effect. Phys Rev B 2000;61:10267.
[6] Kitaev AY. Unpaired Majorana fermions in quantum wires. Phys Usp 2001;44:131–6.
[7] Fu L, Kane CL. Probing neutral Majorana fermion edge modes with charge transport. Phys Rev Lett 2009;102:216403.

[8] Akhmerov AR, Nilsson J, Beenakker CWJ. Electrically detected interferometry of Majorana fermions in a topological insulator. Phys Rev Lett 2009;102:216404.
[9] Law KT, Lee PA, Ng TK. Majorana fermion induced resonant Andreev reflection. Phys Rev Lett 2009;103:237001.
[10] Lutchyn RM, Sau JD, Sarma SD. Majorana fermions and a topological phase transition in semiconductor-superconductor heterostructures. Phys Rev Lett 2010;105:077001.
[11] Oreg Y, Refael G, Oppen FV. Helical liquids and Majorana bound states in quantum wires. Phys Rev Lett 2010;105:177002.
[12] Qi XL, Hughes TL, Zhang SC. Chiral topological superconductor from the quantum Hall state. Phys Rev B 2010;82:184516.
[13] Nadj-Perge S, Drozdov IK, Bernevig BA, et al. Proposal for realizing Majorana fermions in chains of magnetic atoms on a superconductor. Phys Rev B 2013;88:020407.
[14] Li J, Neupert T, Wang ZJ, et al. Two-dimensional chiral topological superconductivity in Shiba lattices. Nat Commun 2016;7:12297.
[15] Mourik V, Zuo K, Frolov SM, et al. Signatures of Majorana fermions in hybrid superconductor-semiconductor nanowire devices. Science 2012;336:1003–7.
[16] Wang MX, Liu CH, Xu JP, et al. The coexistence of superconductivity and topological order in the Bi_2Se_3 thin films. Science 2012;336:52–5.
[17] Nadj-Perge S, Drozdov IK, Li J, et al. Observation of Majorana fermions in ferromagnetic atomic chains on a superconductor. Science 2014;346:602–7.
[18] Deng MT, Vaitiekenas S, Hansen EB, et al. Majorana bound state in a coupled quantum-dot hybrid-nanowire system. Science 2016;354:1557–62.
[19] Albrecht SM, Higginbotham AP, Madsen M, et al. Exponential protection of zero modes in Majorana islands. Nature 2016;531:206.
[20] Xu JP, Liu C, Wang MX, et al. Artificial topological superconductor by the proximity effect. Phys Rev Lett 2014;112:217001.
[21] Xu JP, Wang MX, Liu ZL, et al. Experimental detection of a Majorana mode in the core of a magnetic vortex inside a topological insulator-superconductor $Bi_2Te_3/NbSe_2$ heterostructure. Phys Rev Lett 2015;114:017001.
[22] Sun HH, Zhang KW, Hu LH, et al. Majorana zero mode detected with spin selective Andreev reflection in the vortex of a topological superconductor. Phys Rev Lett 2016;116:257003.
[23] Jeon S, Xie Y, Li J, et al. Distinguishing a Majorana zero mode using spin-resolved measurements. Science 2017;358:772–6.
[24] He QL, Pan L, Stern AL, et al. Chiral Majorana fermion modes in a quantum anomalous Hall insulator-superconductor structure. Science 2017;357:294–9.
[25] Zhang H, Liu CX, Gazibegovic S, et al. Quantized majorana conductance. Nature 2018;556:74.
[26] Zhang H, Gül Ö, Conesa-Boj S, et al. Ballistic superconductivity in semiconductor nanowires. Nat Commun 2017;8:16025.
[27] Gül Ö, Zhang H, Bommer JDS, et al. Ballistic Majorana nanowire devices. Nat Nanotechnol 2018;13:192.
[28] Hor YS, Williams AJ, Checkelsky JG, et al. Superconductivity in $Cu_xBi_2Se_3$ and its implications for pairing in the undoped topological insulator. Phys Rev Lett 2010;104:057001.
[29] Wray LA, Xu SY, Xia Y, et al. Observation of topological order in a superconducting doped topological insulator. Nat Phys 2010;6:855–9.
[30] Hosur P, Ghaemi P, Mong RSK, et al. Majorana modes at the ends of superconductor vortices in doped topological insulators. Phys Rev Lett 2011;107:097001.
[31] Wang ZF, Zhang H, Liu D, et al. Topological edge states in a high-temperature superconductor $FeSe/SrTiO_3(001)$ film. Nat Mater 2016;15:968–73.
[32] Chang TR, Chen PJ, Bian G, et al. Topological Dirac surface states and superconducting pairing correlations in $PbTaSe_2$. Phys Rev B 2016;93:245130.
[33] Guan SY, Chen PJ, Chu MW, et al. Superconducting topological surface states in the noncentrosymmetric bulk superconductor $PbTaSe_2$. Sci Adv 2016;2: e1600894.
[34] Sakano M, Okawa K, Kanou M, et al. Topologically protected surface states in a centrosymmetric superconductor β-$PdBi_2$. Nat Commun 2015;6:8595.
[35] Lv YF, Wang WL, Zhang YM, et al. Experimental signature of topological superconductivity and Majorana zero modes on β-Bi_2Pd thin films. Sci Bull 2017;62:852–6.
[36] Iwaya K, Kohsaka Y, Okawa K, et al. Full-gap superconductivity in spin-polarised surface states of topological semimetal β-$PdBi_2$. Nat Commun 2017;8:976.
[37] Zhang JF, Guo PJ, Gao M, et al. β-$RhPb_2$: a topological superconductor candidate. Phys Rev B 2019;99:045110.
[38] Wang Z, Zhang P, Xu G, et al. Topological nature of the $FeSe_{0.5}Te_{0.5}$ superconductor. Phys Rev B 2015;92:115119.
[39] Yin JX, Wu Z, Wang JH, et al. Observation of a robust zero-energy bound state in iron-based superconductor Fe (Te, Se). Nat Phys 2015;11:543.
[40] Wu XX, Qin S, Liang Y, et al. Topological characters in $Fe(Te_{1-x}Se_x)$ thin films. Phys Rev B 2016;93:115129.
[41] Xu G, Lian B, Tang P, et al. Topological superconductivity on the surface of Fe-based superconductors. Phys Rev Lett 2016;117:047001.
[42] Zhang P, Yaji K, Hashimoto T, et al. Observation of topological superconductivity on the surface of an iron-based superconductor. Science 2018;360:182.
[43] Wang DF, Kong LY, Fan P, et al. Evidence for Majorana bound states in an iron-based superconductor. Science 2018;362:333.
[44] Kong LY, Zhu SY, Papaj M, et al. Observation of half-integer level shift of vortex bound states in an iron-based superconductor. arXiv:1901.02293, 2019.
[45] Machida T, Sun Y, Pyon S, et al. Zero-energy vortex bound state in the superconducting topological surface state of Fe (Se, Te). arXiv:1812.08995, 2018.
[46] Kong LY, Ding H. Majorana gets an iron twist. Natl Sci Rev 2019;6:196–7.
[47] Hao N, Hu JP. Topological quantum states of matter in iron-based superconductors: from concept to material realization. Natl Sci Rev 2019;6:213–26.
[48] Jiang K, Dai X, Wang ZQ. Quantum anomalous vortex and Majorana zero mode in iron-based superconductor Fe(Te, Se). Phys Rev X 2019;9:011033.
[49] Zhang P, Wang Z, Wu X, et al. Multiple topological states in iron-based superconductors. Nat Phys 2019;15:41–7.
[50] Rameau JD, Zaki N, Gu GD, et al. On the interplay of paramagnetism and topology in the Fe-based high T_c superconductors. arXiv:1903.10344, 2019.
[51] Shi X, Han ZQ, Richard P, et al. $FeTe_{1-x}Se_x$ monolayer films: towards the realization of high-temperature connate topological superconductivity. Sci Bull 2019;62:503–7.
[52] Peng XL, Li Y, Wu XX, et al. Observation of topological transition in high-T_c superconductor $FeTe_{1-x}Se_x/SrTiO_3(001)$ monolayers. arXiv:1903.05968, 2019.
[53] Liu Q, Chen C, Zhang T, et al. Robust and clean Majorana zero mode in the vortex core of high-temperature superconductor $(Li_{0.84}Fe_{0.16})OHFeSe$. Phys Rev X 2018;8:041056.
[54] Takei S, Fregoso BM, Hui HY, et al. Soft superconducting gap in semiconductor Majorana nanowires. Phys Rev Lett 2013;110:186803.
[55] Rainis D, Loss D. Majorana qubit decoherence by quasiparticle poisoning. Phys Rev B 2012;85:174533.
[56] Colbert JR, Lee PA. Proposal to measure the quasiparticle poisoning time of Majorana bound states. Phys Rev B 2014;89:140505.
[57] Herrera E, Guillamón I, Galvis JA, et al. Magnetic field dependence of the density of states in the multiband superconductor β-$PdBi_2$. Phys Rev B 2015;92:054507.
[58] Imai Y, Nabeshima F, Yoshinaka T, et al. Superconductivity at 5.4 K in β-Bi_2Pd. J Phys Soc Jpn 2012;81:113708.
[59] Denisova NV, Matetskiya AV, Tupkaloa AV, et al. Growth of layered superconductor β-$PdBi_2$ films using molecular beam epitaxy. Appl Surf Sci 2017;401:142–5.
[60] Li YY, Wang G, Zhu XG, et al. Intrinsic topological insulator Bi_2Te_3 thin films on Si and their thickness limit. Adv Mater 2010;22:4002.
[61] Zhang Y, He K, Chang CZ, et al. Crossover of the three-dimensional topological insulator Bi_2Se_3 to the two-dimensional limit. Nat Phys 2010;6:584–8.
[62] Balatsky AV, Lee WS, Shen ZX. Bogoliubov angle, particle-hole mixture, and angle-resolved photoemission spectroscopy in superconductors. Phys Rev B 2009;79:020505.
[63] Matsui H, Sato T, Takahashi T, et al. BCS-like Bogoliubov quasiparticles in high-T_c superconductors observed by angle-resolved photoemission spectroscopy. Phys Rev Lett 2003;90:217002.
[64] Campuzano JC, Ding H, Norman MR, et al. Direct observation of particle-hole mixing in the superconducting state by angle-resolved photoemission. Phys Rev B 1996;53:737.
[65] Mou DX, Jiang R, Taufour V, et al. Momentum dependence of the superconducting gap and in-gap states in MgB_2 multiband superconductor. Phys Rev B 2015;91:214519.
[66] Zhang WT, Bok JM, Yun JH, et al. Extraction of normal electron self-energy and pairing self-energy in the superconducting state of the $Bi_2Sr_2CaCu_2O_8$ superconductor via laser-based angle-resolved photoemission. Phys Rev B 2012;85:064514.
[67] Reber TJ, Plumb NC, Cao Y, et al. Prepairing and the "filling" gap in the cuprates from the tomographic density of states. Phys Rev B 2013;87:060506.
[68] He JF, Rotundu CR, Scheurer MS, et al. Fermi surface reconstruction in electron-doped cuprates without antiferromagnetic long-range order. Proc Natl Acad Sci USA 2019;116:3449.
[69] Gor'kov LP, Rashba EI. Superconducting 2D system with lifted spin degeneracy: mixed singlet-triplet state. Phys Rev Lett 2001;87:037004.
[70] Mizushima T, Yamakage A, Sato M, et al. Dirac-fermion-induced parity mixing in superconducting topological insulators. Phys Rev B 2014;90:184516.
[71] Fu L, Berg E. Odd-parity topological superconductors: theory and application to $Cu_xBi_2Se_3$. Phys Rev Lett 2010;105:097001.
[72] Wang BT, Margine ER. Evolution of the topologically protected surface states in superconductor β-Bi_2Pd from the three-dimensional to the two-dimensional limit. J Phys Condens Matter 2017;29:325501.

Jian-Yu Guan obtained her B.S. degree from Inner Mongolia University in 2014, and now is a Ph.D. student at Institute of Physics, Chinese Academy of Sciences, supervised by Profs. Hong Ding and Yu-Jie Sun. Her research interests focus on strongly correlated electronic materials, 2D transition metal oxide films and interfacial materials.

Yu-Jie Sun obtained his B.S. degree and Ph.D. degree (2009) from the Tsinghua University. He then worked in Brookhaven National Laboratory as a visiting scientist before joining the Institute of Physics, Chinese Academy of Sciences in 2013. His research interests focus on the synthesis of high temperature superconductors, superlattice, combinatorial films and interface superconductors by molecular beam epitaxy (MBE) and discovery of new superconductor.

Hong Ding obtained his B.S. degree from Shanghai Jiao Tong University in 1990 and Ph.D. degree from the University of Illinois at Chicago in 1995. He then worked at Argonne National Laboratory and Boston College before joining the Institute of Physics, Chinese Academy of Sciences in 2008. His current research interests focus on high temperature superconductors such as cuprate and iron-based superconductors, superconducting topological systems and Majorana quasiparticles.